

# New rat model of spinal cord infarction with long-lasting functional disabilities generated by intraspinal injection of endothelin-1

Masayuki Otani <sup>1,2</sup>, Yoshihiro Kushida,<sup>2</sup> Yasumasa Kuroda,<sup>2</sup> Shohei Wakao,<sup>2</sup> Yo Oguma,<sup>2</sup> Keisuke Sasaki,<sup>3</sup> Shintaro Katahira,<sup>1</sup> Ryohei Terai,<sup>2</sup> Rie Ryoke,<sup>4</sup> Hiroi Nonaka,<sup>4</sup> Ryuta Kawashima,<sup>4</sup> Yoshikatsu Saiki,<sup>1</sup> Mari Dezawa<sup>2</sup>

**To cite:** Otani M, Kushida Y, Kuroda Y, *et al.* New rat model of spinal cord infarction with long-lasting functional disabilities generated by intraspinal injection of endothelin-1. *Stroke & Vascular Neurology* 2024;**0**; doi:10.1136/svn-2023-002962

► Additional supplemental material is published online only. To view, please visit the journal online (<https://doi.org/10.1136/svn-2023-002962>).

Received 4 November 2023

Accepted 4 June 2024



© Author(s) (or their employer(s)) 2024. Re-use permitted under CC BY-NC. No commercial re-use. See rights and permissions. Published by BMJ.

<sup>1</sup>Division of Cardiovascular Surgery, Tohoku University Graduate School of Medicine, Sendai, Miyagi, Japan

<sup>2</sup>Department of Stem Cell Biology and Histology, Tohoku University Graduate School of Medicine, Sendai, Miyagi, Japan

<sup>3</sup>Department of Neurosurgery, Tohoku University Graduate School of Medicine, Sendai, Miyagi, Japan

<sup>4</sup>Institute of Development, Aging, and Cancer, Tohoku University, Sendai, Miyagi, Japan

**Correspondence to**  
Dr Masayuki Otani;  
otani817@gmail.com

Dr Mari Dezawa;  
mdezawa@med.tohoku.ac.jp

Dr Yoshikatsu Saiki;  
yoshisaiki@med.tohoku.ac.jp

## ABSTRACT

**Background** The current method for generating an animal model of spinal cord (SC) infarction is highly invasive and permits only short-term observation, typically limited to 28 days.

**Objective** We aimed to establish a rat model characterised by long-term survival and enduring SC dysfunction by inducing selective ischaemic SC damage.

**Methods** In 8-week-old male Wistar rats, a convection-enhanced delivery technique was applied to selectively deliver endothelin-1 (ET-1) to the anterior horn of the SC at the Th13 level, leading to SC infarction. The Basso, Beattie and Bresnahan (BBB) locomotor score was assessed for 56 days. The SC was examined by a laser tissue blood flowmeter, MRI, immunohistochemistry, triphenyl tetrazolium chloride (TTC) staining, Western blots and TUNEL staining.

**Results** The puncture method was used to bilaterally inject 0.7 µL ET-1 (2.5 mg/mL) from the lateral SC into the anterior horns (40° angle, 1.5 mm depth) near the posterior root origin. Animals survived until day 56 and the BBB score was stably maintained (5.5±1.0 at day 14 and 6.2±1.0 at day 56). Rats with BBB scores ≤1 on day 1 showed stable scores of 5–6 after day 14 until day 56 while rats with BBB scores >1 on day 1 exhibited only minor dysfunction with BBB scores >12 after day 14. TTC staining, immunostaining and TUNEL staining revealed selective ischaemia and neuronal cell death in the anterior horn. T2-weighted MR images showed increasing signal intensity at the SC infarction site over time. Western blots revealed apoptosis and subsequent inflammation in SC tissue after ET-1 administration.

**Conclusions** Selective delivery of ET-1 into the SC allows for more precise localisation of the infarcted area at the targeted site and generates a rat SC infarction model with stable neurological dysfunction lasting 56 days.

## INTRODUCTION

Spinal cord (SC) infarction may be caused by arteriosclerosis, aortic surgery or vertebral artery dissection and occasionally leads to serious complications such as paraplegia.<sup>1</sup> No established therapies exist for SC infarction. Animal models of SC infarction are generally created by temporarily occluding

## WHAT IS ALREADY KNOWN ON THIS TOPIC

⇒ Current animal models of spinal cord (SC) infarction are created by blocking aortic blood flow using forceps and balloons, which leads to a high mortality rate due to abdominal organ ischaemia and a short observation period of only 7–28 days. Adequate evaluation of functional recovery requires an extended survival period.

## WHAT THIS STUDY ADDS

⇒ Injection of endothelin-1 into the anterior horns at a targeted SC level using a convection-enhanced delivery technique induces precise localisation of SC ischaemia and neuronal cell death with a stably maintained motor assessment (Basso, Beattie and Bresnahan, BBB) score of 5–6 until day 56. Rats with a BBB score ≤1 on day 1 showed stable SC dysfunction (BBB score 5–6) until day 56 while those with a BBB score >1 showed only minor dysfunction, suggesting that the BBB score on day 1 is predictive of later scores and allowing for selection of model animals at an earlier time point.

## HOW THIS STUDY MIGHT AFFECT RESEARCH, PRACTICE OR POLICY

⇒ The development of effective therapies requires the availability of a feasible SC infarction model. Our technique induces SC infarction at the targeted site without concern over the influence of SC artery course variations. This model is applicable for inducing SC infarction at various SC segments. Furthermore, reproducible and stable long-lasting neurological dysfunction is maintained for at least 56 days, making our method useful for long-term evaluation of SC infarction.

the descending thoracic or abdominal aorta.<sup>2–6</sup> Despite the relatively short blood flow blockade (~20 min), many animals die within 24 hours due to intestinal necrosis and haematuria caused by abdominal organ ischaemia,<sup>7</sup> allowing only a short observation period (7–28 days).<sup>4 5 8–11</sup> Adequate evaluation of functional SC recovery requires longer

observation periods. Shortening the blood flow interruption to minimise abdominal organ damage, however, decreases the likelihood of adequate SC infarction. We developed an animal model of SC infarction without interrupting aortic blood flow that survived 56 days with stable long-term SC dysfunction online supplemental file 1.

## MATERIALS AND METHODS

### Animals

All animals were cared for in accordance with the Code of Ethics of the World Medical Association and Tohoku University guidelines (2020MdA-146). Adult male Wister rats (175–223g, 8 weeks old, Japan SLC, Hamamatsu, Japan) were single-housed at 22–25°C with a 12-hour light-dark cycle (lights on at 8:00 hours) and provided food and water ad libitum.

### Convection-enhanced delivery technique

The convection-enhanced delivery (CED) technique for inducing SC infarction was established by modifying previously reported methods.<sup>12 13</sup> Briefly, a syringe pump (Pump 11 Elite, HARVARD APPARATUS, Boston, Massachusetts, USA) containing a 10 µL Hamilton syringe was used to inject the solution. The syringe was connected to polyethylene tubing (6010–35606; inner diameter, 250 µm, GL Sciences, Tokyo, Japan), a 27G needle, and fused silica tubing (TSP100170; inner/outer diameter, 100/170 µm, Molex, Lisle, Illinois, USA) (figure 1A, B).

Rats were anaesthetised with isoflurane (5% induction, 2% maintenance), fixed to a stereotactic frame (NARISHIGE, Tokyo, Japan), and body temperature was maintained at 36°C–37°C with a heating pad (BWT-100A, Bio Research Center, Nagoya, Japan). Rats were placed in a prone position, the dorsal hair removed and surgery was performed under a microscope (SZ61, Olympus, Tokyo, Japan). A dorsal 3 cm midline incision exposed the Th12–L1 spinal processes. After Th13 laminectomy, the dura mater and arachnoid were punctured using the 27G needle tip. The puncture site was the lateral cord slightly ventral to the posterior root origin. The fused silica tubing (1.5 mm) was inserted through the hole (figure 1C–E, online supplemental movie 1).

The optimal needle (angle X) angle was determined by injecting 4.0% Evans blue (056–04061, FUJIFILM, Tokyo, Japan) in phosphate-buffered saline (PBS) (figure 1F–I) at 0.2 µL/min. Rats were killed by isoflurane overdose. The SC was dissected out and fixed with 4% paraformaldehyde in PBS. Cross-sections of the puncture site were observed under a microscope (Stemi 305, ZEISS, Oberkochen, Germany).

### Stereotaxic injection of ET-1

Endothelin-1 (1–3 mg/mL solutions in saline, ET-1; E7764, MilliporeSigma, St. Louis, Missouri, USA)<sup>14</sup> was injected at 0.2 µL/min. The needle tip was held stationary for 5 min and slowly withdrawn over 1 min. The muscle lateral to the puncture site was marked by

8–0 monofilament suture. After confirming haemostasis, the erector spinae muscle and skin were sutured. Manual pressure was applied to assist with urination until animals regained the ability to urinate.

### Behavioural assessment

Open-field locomotor function was evaluated using the Basso, Beattie, Bresnahan (BBB) locomotor scale.<sup>15 16</sup> The average score for hindlimb motor function on both the left and right sides was recorded before surgery, at 2 hours after surgery, on days 1, 3, 5, 7, and weekly thereafter to day 56 after surgery until their death.

### SC blood flow measurements before and after ET-1 administration

Referring to the literature,<sup>17 18</sup> changes in SC blood flow before and after ET-1 administration were evaluated using a laser tissue blood flowmeter (FLO-N1; Omega-wave, Tokyo, Japan). Detailed methods are provided in online supplemental material.

### Immunofluorescence staining

Rats were killed by isoflurane overdose and perfused intracardially with PBS followed by 4% paraformaldehyde in PBS. SCs were removed and postfixed overnight at 4°C in 4% paraformaldehyde. Tissues were immersed overnight in 15%, 20% and 25% sucrose in PBS at 4°C, embedded in Tissue-Tek OCT Compound (4583, SAKURA, Tokyo, Japan) and cut into cryosections (~7 µm thick). Sections were incubated in blocking solution containing 20% BlockAce (UKB40, KAC, Kyoto, Japan), 5% bovine serum albumin (01860-65, Nacalai Tesque, Kyoto, Japan) and 0.3% Triton X-100 (168-11805, Fuji-film) in PBS for 30 min, followed by incubation with rabbit anti-NeuN (1:500; ab177487, Abcam, Cambridge, England), goat anti-Iba1 (1:500; ab5076, Abcam), mouse anti-GFAP (1:500; G3893, MilliporeSigma), rabbit anti-GST-pi (1:200; 312, MBL, Tokyo, Japan) or anti-endothelial cell (EC) antibody (RECA-1; 1:100; ab9774, Abcam) overnight at 4°C. Sections were washed with PBS, followed by incubation with a 1:200 dilution of Alexa Fluor 488-conjugated donkey anti-goat IgG, anti-mouse IgG or anti-rabbit IgG (705-545-003, 715-546-150, 711-586-152, respectively, Jackson ImmunoResearch, Philadelphia, Pennsylvania, USA), combined with a 1:500 dilution of 4',6-diamidino-2-phenylindole (DAPI; D9542, MilliporeSigma) for 2 hours at room temperature. The samples were washed in PBS, covered with SlowFade Gold antifade reagent (S36937, Life Technology, Carlsbad, California, USA) and examined under a laser confocal microscope (Eclipse Ti, Nikon, Tokyo, Japan).

Six areas (200×200 µm/field) and 10 areas (150×150 µm/field) from cross sections obtained at the puncture level were randomly selected from the anterior and posterior horns for staining with NeuN and TUNEL, respectively, and 10 areas (150×150 µm/field) from the grey and white matter of the ventral and dorsal sides for

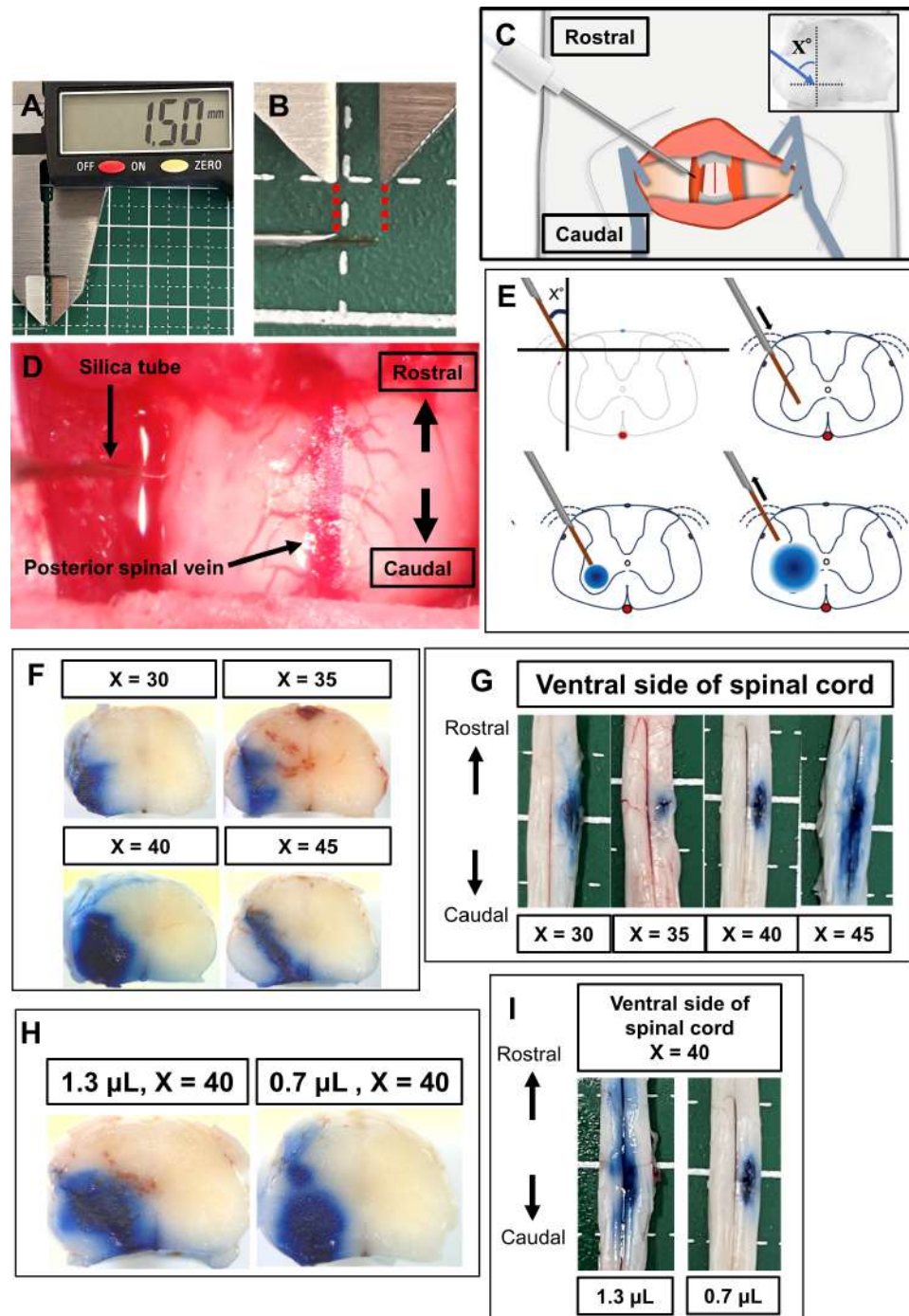


**Figure 1** (A, B) The length of the silica tubing was adjusted to 1.5 mm using a digital calliper. (C) Schematic diagram of the intraoperative view. (D) Intraoperative picture under the microscope (see online supplemental movie 1). (E) Schematic diagram of the Evans blue injection centred on the anterior horn of the spinal cord (SC). (F) Representative example of Evans blue administration (0.7  $\mu\text{L}$ ) at angle X. (G) Overall image of the ventral side of the SC injected with 0.7  $\mu\text{L}$  of Evans blue at each angle. (H) Diffusion of the dye in the SC, with 1.3 and 0.7  $\mu\text{L}$  Evans blue. (I) Diffusion of the dye in the ventral SC was observed for two different volumes: 1.3  $\mu\text{L}$  and 0.7  $\mu\text{L}$ .

RECA-1. Positive cells were counted to calculate the cell number per unit area ( $\text{cells}/\text{mm}^2$ ).

#### Triphenyl tetrazolium chloride staining

Triphenyl tetrazolium chloride (TTC) staining was performed as previously described.<sup>19–21</sup> SCs, collected at 7 days after ET-1 injection, were sliced into 3.0 mm thick

axial sections, incubated in 2% TTC dissolved in PBS for 30 min at 37°C, and fixed with 4% paraformaldehyde in PBS. SCs from intact rats were also stained.

#### TUNEL assay

The TUNEL assay was performed using an in situ cell death detection kit (TMR Red, Roche Diagnostics, Basel,

Switzerland) according to the manufacturer's instructions. For the negative control, label solution was used instead of the TUNEL reaction mixture. An intact SC treated with DNase was used as the positive control.

### Statistical analysis

Statistical analyses were performed using GraphPad Prism (V.10.0.2, GraphPad Software, San Diego, California, USA). Results are presented as mean±SEM. Data were analysed by two-way analysis of variance, followed by multiple comparisons using Tukey's HSD for comparing more than two groups. Student's t-test was used to compare two groups. A  $p < 0.05$  was considered to indicate statistical significance.

## RESULTS

### Puncture angle optimisation

Critical segmental arteries are present at Th10 to L2 in rats.<sup>22</sup> Therefore, we targeted Th13 for our SC infarction model. When injecting 0.7 µL Evans blue, the angle formed by the silica tube and dorsoventral axis (X) was set to 30° (n=3), 35° (n=3), 40° (n=8) or 45° (n=10). SCs were removed 1 hour later and inspected (figure 1F). Evans blue mainly remained in the anterior horn at X=40 and was located in the outer white matter at X=30, in both the outer white matter and anterior horn at X=35 and leaked into areas around the anterior spinal artery at X=45 (figure 1F). Images of the ventral SC for injections given at each angle are shown in (figure 1G). At X=30 and X=45, the dye spread in the rostral and caudal directions from the injection site, with a more extended reach to the anterior spinal artery areas at X=45 (figure 1F). At X=35 and X=40, the dye remained on the side ipsilateral to the injection. Thus, the X=40 puncture angle was used in the following experiments.

### Injection volume optimisation

Evans blue (0.7 or 1.3 µL/injection) was injected and rats were killed 1 hour later. Dye diffusion was observed in cross-sections (figure 1H) and the ventral SC (figure 1I). In the cross-sections, the dye remained within the grey matter, particularly the anterior horn, under both conditions. On the ventral SC, however, the 0.7 µL injection remained on the ipsilateral side and the 1.3 µL injection spread to the contralateral side. Thus, 0.7 µL injections were used in the following experiments.

### Optimisation of the ET-1 concentration

In the SC contusion model, the BBB score is generally 5–6 at 14 days.<sup>23 24</sup> A score  $\geq 9$  is considered to indicate mild symptoms with the ability to bear a hindlimb load while scores of 0–1 indicate severe impairment. Thus, we aimed to generate an SC infarction model with a stable BBB score of 5–6 after day 14, similar to the SC contusion model.

To optimise the ET-1 concentration, we injected 0.7 µL ET-1 at a concentration of 1.0, 2.0, 2.5 or 3.0 mg/mL bilaterally into the SC anterior horn online supplemental file

2. The BBB score on day 14 was  $12.8 \pm 0.8$  at 1.0 mg/mL,  $9.3 \pm 1.3$  at 2.0 mg/mL,  $5.5 \pm 1.0$  at 2.5 mg/mL, and  $4.2 \pm 2.5$  at 3.0 mg/mL (figure 2A). Thus, we injected 2.5 mg/mL ET-1 for the following studies.

In summary, 0.7 µL ET-1 (2.5 mg/mL) was injected into the SC bilaterally at Th13 with a puncture angle of 40° at a 1.5 mm depth to generate the SC infarction model (ET-1 group).

### BBB locomotor scale

The BBB score of the ET-1 (n=20), control (0.7 µL PBS; n=12) and sham (silica tube puncture only; n=7) groups was evaluated until day 56 (figure 2B). In contrast to the ET-1 group, the control and sham groups showed a slightly decreased BBB score after treatment followed by recovery to baseline by day 7. No deaths occurred in the control and sham groups. In the ET-1 group, 39.4% (n=13) of the rats died (urinary dysfunction in 9, unknown in 4) and their data are excluded from the graph. Mean time to death was  $9.9 \pm 1.8$  days. From day 14 to 56, the BBB score in the ET-1 group remained stable, 5.5–6.2, and was significantly lower than that of the control and sham groups (figure 2B,  $p < 0.01$ ).

The ET-1 group was divided into two groups based on the BBB score on day 1: severe ET-1 group (BBB score  $\leq 1$  on day 1) and Mild ET-1 group (BBB score  $> 1$  on day 1; figure 2C). Throughout the observation period, the BBB score differed significantly between the severe and mild groups ( $p < 0.01$ , from day 1 to day 56). Selecting rats with BBB scores ranging from 0 to 1 on day 1 increased the likelihood of excluding individuals with minor SC dysfunction and obtaining stable SC infarction models. At day 56, the BBB score of the total ET-1 group was  $6.2 \pm 1.0$ , whereas that of the mild group was  $13.3 \pm 0.3$  and that of the severe group was  $4.9 \pm 0.9$ .

### Body weight changes

Body weight was monitored in the sham, control and mild and severe ET-1 groups until day 56. Body weight was normalised to the mean preoperative weight. At day 1, the severe ET-1 group exhibited significantly greater weight loss than the sham and control groups ( $p < 0.05$  vs sham;  $p < 0.01$  vs control). Normalised body weight in the Mild group did not differ significantly from that of the other groups. From days 3 to 7, body weight did not differ significantly between the severe and mild groups, and both groups were underweight compared with the sham and control groups ( $p < 0.01$ ). On day 14, the mild group normalised body weight recovered and did not differ significantly among the mild, sham and control groups after day 21 while the severe group remained significantly underweight compared with the other 3 groups after day 21 (severe group vs other groups;  $p < 0.01$ ).

### TTC staining

Compared with intact SC at the Th13 level, the ET-1 group at day 7 exhibited a whitish ischaemic region mainly in the anterior horn at the same SC level (figure 3A).

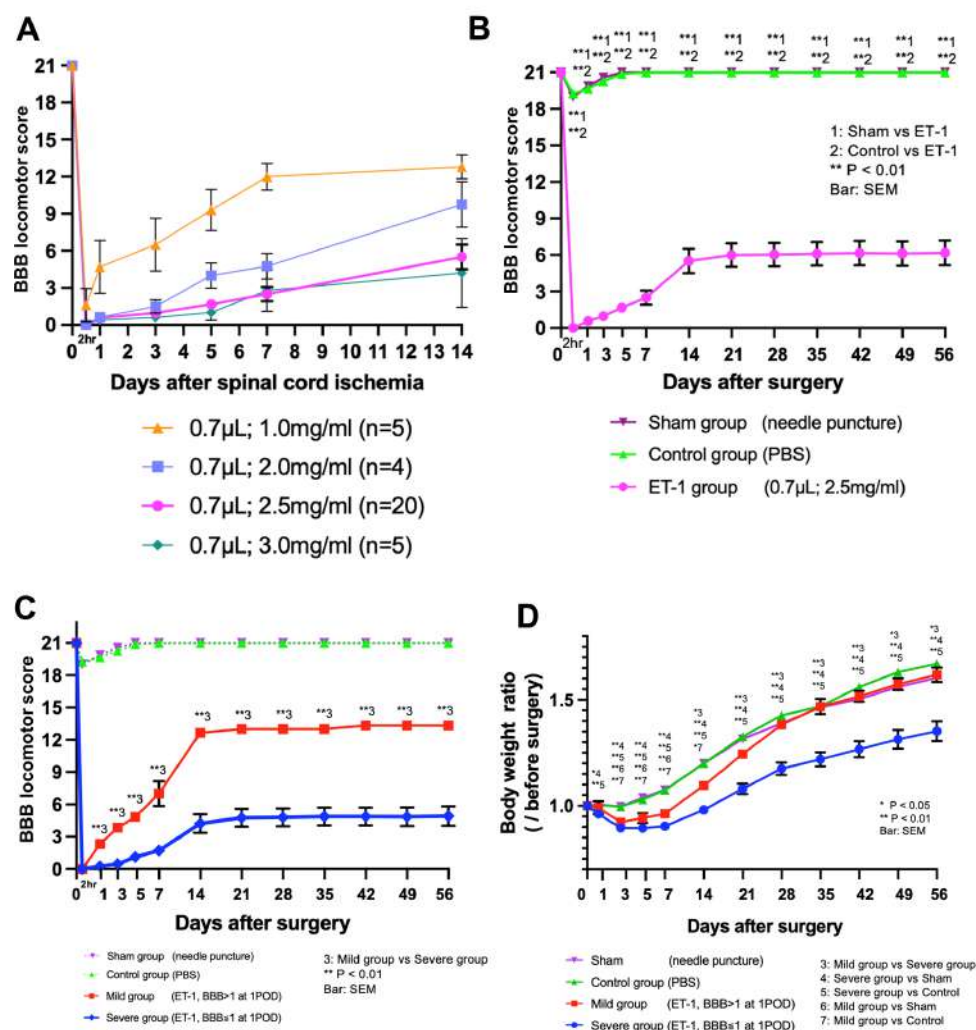


**Figure 2** Changes in the BBB locomotor score and body weight ratio. (A) The volume of ET-1 was fixed at 0.7  $\mu$ L/side, and the concentration was varied. Each rat was observed for 14 days, and mortality rates are shown below: all five rats/group administered 1.0mg/mL and 3.0mg/mL ET-1, respectively, survived for 14 days; 1 of the 5 rats administered 2.0mg/mL ET-1 died on day 4, and the other rats survived for 14 days. Data for the rat that died during the observation period were excluded from the graph. (B) ET-1 (0.7  $\mu$ L/side, 2.5mg/mL) was injected. (C) The BBB score on postoperative day 1 predicted the BBB score in the chronic phase. At 2 hours postoperatively, both the severe and mild groups had a BBB score of 0. Already on day 1 after the injection, however, the BBB score differed significantly, with the severe group having a mean BBB score of  $0.26 \pm 0.10$  and the Mild group having a BBB score of  $2.33 \pm 0.36$  ( $p < 0.01$ ). (D) The body weight changes in each group up to day 56. The average preoperative weight was defined as 1.0. BBB, Basso, Beattie and Bresnahan; PBS, phosphate-buffered saline.

### Vasoconstriction process after ET-1 injection

The blood flow was significantly decreased immediately, 15 min and 30 min after ET-1 administration compared with that before ET-1 administration (figure 3B, before vs just after;  $p < 0.001$ , before vs 15 min;  $p < 0.001$ , before vs 30 min;  $p < 0.05$ ). After 60 min, blood flow improved to the same level as before ET-1 administration (Before vs 60 min; not significant).

### Immunohistochemical analysis

Expression of NeuN and inflammation markers Iba-1, GFAP and GST-pi in the SC at Th13 was examined in the intact and ET-1 groups at day 3 (acute phase) and day 56 (chronic phase; figure 3C). Positive and

negative controls for each marker are shown in online supplemental file 5. The number of NeuN-positive cells was reduced primarily in the anterior horn of the ET-1- (day 3) and ET-1- (day 56) groups compared with the intact group while the number of Iba-1-positive cells tended to be higher in the ET-1- (day 3) group compared with the intact and ET-1- (56 days) groups. GFAP, predominantly expressed in the white matter in the intact and ET-1- (day 3) groups, was observed in both the white and grey matter in the ET-1- (day 56) group. Consistent with a previous report that the oligodendrocyte number is reduced in ischaemic brain,<sup>25</sup> GST-pi-positivity in the grey matter

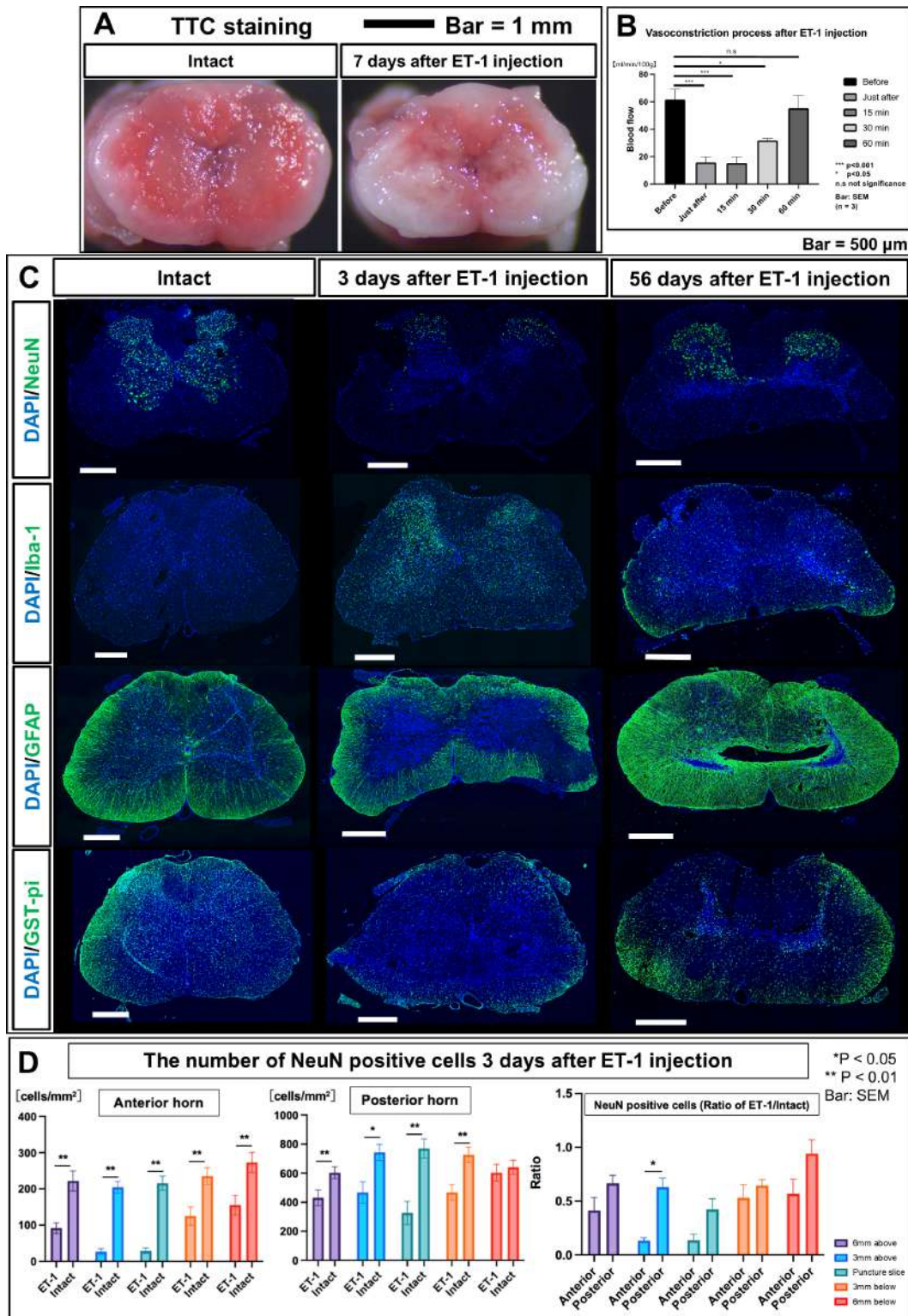


**Figure 3** (A) TTC staining. Left: intact spinal cord (SC) at the Th13 level. Right: punctured cross-section on day 7n in the ET-1 group. (B) Vasoconstriction process after ET-1 injection. Blood flow at the level of Th13 was  $61.6 \pm 7.4$  mL/min/100g before ET-1 administration,  $15.9 \pm 4.0$  mL/min/100g immediately after ET-1 administration,  $15.3 \pm 4.3$  mL/min/100g at 15 min,  $31.9 \pm 1.4$  mL/min/100g at 30 min and  $55.3 \pm 9.0$  mL/min/100g at 60 min. The blood flow was significantly decreased immediately, 15 min and 30 min after ET-1 administration compared with that before ET-1 administration (before vs just after;  $p < 0.001$ , before vs 15 min;  $p < 0.001$ , before vs 30 min;  $p < 0.05$ ). After 60 min, blood flow improved to the same level as before ET-1 administration (before vs 60 min; not significant). (C) Immunostaining with neurological markers, NeuN, Iba-1, GFAP and GST-pi. (D) Number of NeuN positive cells 3 days after ET-1 injection compared with intact SC. TTC, triphenyl tetrazolium chloride.

was reduced by the ischaemic damage in ET-1 (day 3) and ET-1- (day 56) groups (figure 3C).

We counted the number of NeuN(+) cells in the SC grey matter, focusing on the comparison between the ET-1- (day 3) and intact groups. Cross-sections were made at five levels: the puncture level, and at 6 mm and 3 mm rostral, and 3 mm and 6 mm caudal levels. At all five levels, cell numbers were significantly lower in the anterior horn of the ET-1- (day 3) group than in the intact group ( $p < 0.01$ ; figure 3D). In the cross-section of the puncture level, the ratio of ET-1/intact cells showed that the NeuN-positive cell number in the anterior and posterior horns of the ET-1 group was  $13.5\% \pm 5.7\%$  and  $42.3\% \pm 9.9\%$ , respectively, that of the intact group. In the 3 mm rostral section, the NeuN (+) cell number was significantly decreased in the anterior horn compared with the posterior horn.

#### TUNEL-positive cells in the anterior and posterior horns

Cell death induced by ET-1 injection in the grey matter of the ET-1- (day 3) group was examined. The positive and negative controls for TUNEL staining are shown in online supplemental file 5. The number of TUNEL-positive cells was significantly higher in the anterior horn than in the posterior horn ( $168.9 \pm 22.7$  vs  $34.4 \pm 7.3$ ,  $p < 0.01$ ; figure 4A). In the TUNEL/NeuN-double staining, 14.8% of TUNEL-positive cells were NeuN-positive, suggesting that ET-1-induced SC infarction led to NeuN-positive cell death (figure 4B).

#### RECA-1-positive vessels in the SC

The effect of ET-1 on the number of SC vessels was examined by counting the number of RECA-1 (+) vessels in the grey and white matter at the puncture level in the ET-1- (day 3) and intact groups at the Th13 level (figure 4C). Therefore, the number of RECA-1-positive vessels in the grey matter and ventral white matter at the level of the injection did not differ significantly between the ET-1- (day 3) and intact groups. On the other hand, the number of RECA-1-positive vessels in the dorsal white matter was significantly higher in the ET-1- (day 3) group than in the intact group (figure 4D).

#### DISCUSSION

We developed a novel rat SC infarction model induced by local ET-1 injection. This is the first report of an SC infarction model in which severe hindlimb dysfunction based on the BBB score and a decreased number of NeuN-positive neuronal cells was maintained for a relatively long period (56 days). Injection of ET-1 into the anterior horn induced a localised SC lesion leading to neuronal cell death predominantly in the anterior horn. Key findings are as follows:

1. The delivery route was optimised for selective injection into the left and right anterior horns of the rat SC 1.5 mm deep from the lateral cord slightly ventral to the posterior root origin.

2. Local injection of ET-1 (0.7  $\mu$ L, 2.5 mg/mL) bilaterally into the anterior horn produced persistent and stable SC dysfunction for up to 56 days.
3. BBB scores on the first postoperative day predicted the BBB score at 56 days postsurgery.
4. The majority of the neuronal cell death based on TUNEL-positive/NeuN-positive staining occurred in the anterior horn compared with the posterior horn.
5. Vessel number in the grey matter on day 3 did not differ significantly between the ET-1 and intact groups, whereas the vessel number in the white matter increased in the ET-1 group compared with the intact group.

Many studies reporting SC infarction induced by aortic occlusion have a short observation time—the longest being 28 days.<sup>26</sup> Few reports include in-depth neurological and histological analyses with long-term follow-up. The success of the aortic clamp model largely depends on the location of the Adamkiewicz artery.<sup>22 27</sup> The present SC infarction model can be stably generated independent of the vascular course.

An ideal experimental model has a repeatable and stable outcome with little variability. In this study, the 21-point BBB scale<sup>15 16</sup> was used as an index of function. The BBB score of an ideal paraplegia model would be  $< 8$ . Our method of inducing SC infarction resulted in a BBB score of  $5.5 \pm 1.0$  at day 14 and  $6.2 \pm 1.0$  at day 56. Importantly, the BBB score on day 1 predicted the score in the chronic phase. These findings indicate the usefulness of this animal model for evaluating SC infarction.

The CED technique involves local injection of small-molecule and large-molecule drugs into a target tissue and is clinically used in brain tumour chemotherapy.<sup>28</sup> We aimed to reach the anterior horn by puncturing from the lateral to the median side of the SC. ET-1, a potent vasoconstrictor and mitogen comprising 21 amino acids initially discovered in ECs,<sup>14</sup> is produced in various cell types. Specific EC agonists trigger the synthesis and release of ET-1, which binds to ET<sub>A</sub><sup>29</sup> and ET<sub>B</sub><sup>30</sup> receptors on vascular smooth muscle cells (VSMCs). While ET<sub>A</sub> receptors are mainly expressed by VSMCs, ET<sub>B</sub> receptors are primarily located in ECs.<sup>31</sup> These Gq-coupled receptors induce VSMC contraction by raising intracellular calcium levels and EC-dependent vasodilation by promoting the release of nitric oxide and prostaglandin I<sub>2</sub>.<sup>32</sup> In the cerebral infarction model induced by the CED technique in mice, both ET-1 and L-NAME are required to induce cerebral ischaemia.<sup>33 34</sup> Because the rat ET receptor isoform differs from that in mice, ET-1 alone is sufficient to induce cerebral infarction. Therefore, in our experiment, SC infarction was successfully induced by injecting only ET-1.

The survival rate was higher in the present study than in previous reports, but 39.4% of the rats ( $n = 13$ ) died during the 56-day observation period. Neurogenic bladder was the cause of death in 9 of 13 rats. Chronic bladder dilation was observed in some rats at 56 days while others exhibited haematuria. These findings indicated the

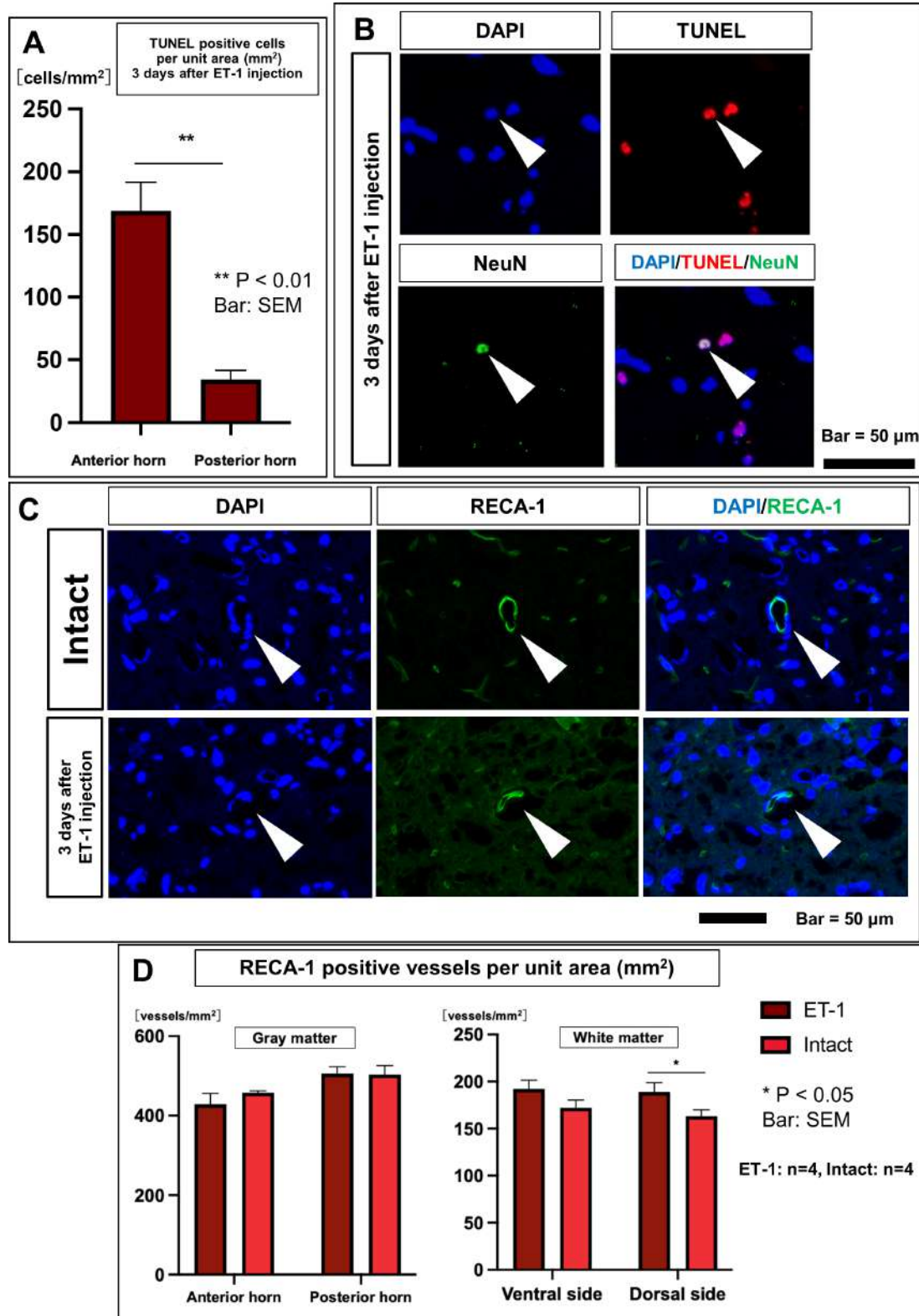


**Figure 4** (A) TUNEL-positive cells per unit area ( $\text{mm}^2$ ) 3 days after ET-1 injection. (B) Double staining with TUNEL and NeuN. (C) Immunostaining for RECA-1. (D) RECA-1 positive vessels per unit area ( $\text{mm}^2$ ). The number of RECA-1 positive vessels ( $/\text{mm}^2$ ) in the anterior horn was  $428.9 \pm 26.9$  and  $457.8 \pm 4.6$  ( $p=0.38$ ) and the number in the posterior horn was  $505.6 \pm 17.6$  and  $503.3 \pm 23.1$  ( $p=0.93$ ) in the ET-1- (day 3) and intact groups, respectively. In the white matter, the number of RECA-1-positive vessels ( $/\text{mm}^2$ ) was  $192.2 \pm 9.2$  and  $172.2 \pm 8.2$  ( $p=0.11$ ) on the ventral side and  $188.9 \pm 10.0$  and  $163.3 \pm 6.6$  ( $p=0.04$ ) on the dorsal side in the ET-1- (day 3) and intact groups, respectively.

persistence of supranuclear lower urinary tract dysfunction in the chronic phase. Daily urinary care is thus necessary for long-term survival, and higher survival rates may be achieved if urinary retention due to neurogenic bladder is relieved.

In the histological evaluation, the significant decrease in NeuN (+) cells at days 3 and 56 was considered to contribute to long-term SC dysfunction. GFAP, an astrocyte marker, was strongly expressed at day 56. Glial scarring in the chronic phase hinders nerve regeneration in central nervous system disorders, and a similar mechanism might have occurred in this model.<sup>35</sup>

Analysis of vascular density revealed a moderate decrease in the number of vessels in the anterior horn on day 3 compared with that in intact SC. In the white matter, the number of vessels tended to increase in both the ventral and dorsal regions in the ET-1 group. This may be due to a compensatory blood supply to the anterior horn through collateral perfusion from surrounding areas.

This model has several advantages. SC infarction can be induced at the targeted site without concern for the course of vessels surrounding the SC. SC infarction in humans is diverse,<sup>26 36</sup> and this model is applicable for inducing SC infarction at various SC segments. The neurological dysfunction was reproducible, stable and long-lasting (56 days). The BBB score in the chronic phase was predicted by that on the first postoperative day.

This model has some limitations. Direct injection of ET-1 into the SC causes minor trauma, and it is important to avoid injuring the posterior spinal artery and vein near the puncture site. Furthermore, although both Evans blue and ET-1 are water-soluble, their penetrability may differ due to variations in the density and diffusion; thus, infusion of Evans blue into the SC may not reflect that of ET-1. In addition, ET-1 has neurotoxic effects associated with inflammatory effects.<sup>37 38</sup> The hindlimb motor dysfunction observed in this model may be due not only to cell death caused by the vasoconstrictive effect of ET-1 in the SC, but also to the inflammatory effects of ET-1 (online supplemental file 6). SC ischaemia causes inflammatory cell infiltration into the grey matter, however, macrophages and microglia are highly upregulated following the expression of inflammatory mediators such as TNF- $\alpha$  and IL-1 $\beta$ .<sup>39</sup> Thus, this model effectively simulates the pathophysiology of SC infarction, capturing the combined effects of ischaemia and inflammation on SC tissue. In summary, we demonstrated that local injection of ET-1 into the anterior horn of the rat SC induces ischaemic injury that results in long-term SC dysfunction until at least day 56. The reproducibility, simplicity and adaptability of this model make it an attractive choice for preclinical studies of SC ischaemic injury.

**Contributors** All listed authors participated in the experiment and approved the submitted manuscript. MD designed the experiments. MO performed the animal experiments, acquired all the data and wrote the draft of the manuscript. YKushida and SW supervised the experimental procedures. KS, SK and RT guided MO in performing the animal experiments. RK, RR and HN provided support for obtaining

magnetic resonance images of the animals. YKuroda and YO assisted with the data analysis. MD and YS acquired the research funding and revised the article. MO, YS and MD were the guarantor to this manuscript.

**Competing interests** None declared.

**Patient consent for publication** Not applicable.

**Provenance and peer review** Not commissioned; externally peer reviewed.

**Data availability statement** All data relevant to the study are included in the article or uploaded as online supplemental information. Not applicable.

**Supplemental material** This content has been supplied by the author(s). It has not been vetted by BMJ Publishing Group Limited (BMJ) and may not have been peer-reviewed. Any opinions or recommendations discussed are solely those of the author(s) and are not endorsed by BMJ. BMJ disclaims all liability and responsibility arising from any reliance placed on the content. Where the content includes any translated material, BMJ does not warrant the accuracy and reliability of the translations (including but not limited to local regulations, clinical guidelines, terminology, drug names and drug dosages), and is not responsible for any error and/or omissions arising from translation and adaptation or otherwise.

**Open access** This is an open access article distributed in accordance with the Creative Commons Attribution Non Commercial (CC BY-NC 4.0) license, which permits others to distribute, remix, adapt, build upon this work non-commercially, and license their derivative works on different terms, provided the original work is properly cited, appropriate credit is given, any changes made indicated, and the use is non-commercial. See: <http://creativecommons.org/licenses/by-nc/4.0/>.

#### ORCID ID

Masayuki Otani <http://orcid.org/0000-0003-1742-0311>

#### REFERENCES

- Weidauer S, Nichtweiß M, Hattingen E, *et al*. Spinal cord ischemia: aetiology, clinical syndromes and imaging features. *Neuroradiology* 2015;57:241–57.
- Zivin JA, DeGirolami U. Spinal cord infarction: a highly reproducible stroke model. *Stroke* 1980;11:200–2.
- Lang-Lazdunski L, Matsushita K, Hirt L, *et al*. Spinal cord ischemia. Development of a model in the mouse. *Stroke* 2000;31:208–13.
- LeMay DR, Neal S, Neal S, *et al*. Paraplegia in the rat induced by aortic cross-clamping: model characterization and glucose exacerbation of neurologic deficit. *J Vasc Surg* 1987;6:383–90.
- Yin F, Guo L, Meng C, *et al*. Transplantation of mesenchymal stem cells exerts anti-apoptotic effects in adult rats after spinal cord ischemia-reperfusion injury. *Brain Res* 2014;1561:1–10.
- Taira Y, Marsala M. Effect of proximal arterial perfusion pressure on function, spinal cord blood flow, and histopathologic changes after increasing intervals of aortic occlusion in the rat. *Stroke* 1996;27:1850–8.
- Kato H, Kanellopoulos GK, Matsuo S, *et al*. Neuronal apoptosis and necrosis following spinal cord ischemia in the rat. *Exp Neurol* 1997;148:464–74.
- Yasuda N, Sasaki M, Kataoka-Sasaki Y, *et al*. Intravenous delivery of mesenchymal stem cells protects both white and gray matter in spinal cord ischemia. *Brain Res* 2020;1747:147040.
- Jing N, Fang B, Li Z, *et al*. Exogenous activation of cannabinoid-2 receptor modulates Tlr4/Mmp9 expression in a spinal cord ischemia reperfusion rat model. *J Neuroinflammation* 2020;17:101.
- Chen S, Yi M, Zhou G, *et al*. Abdominal aortic transplantation of bone marrow mesenchymal stem cells regulates the expression of ciliary neurotrophic factor and inflammatory cytokines in a rat model of spinal cord ischemia-reperfusion injury. *Med Sci Monit* 2019;25:1960–9.
- Kurose T, Takahashi S, Otsuka T, *et al*. Simulated microgravity-cultured mesenchymal stem cells improve recovery following spinal cord ischemia in rats. *Stem Cell Res* 2019;41:101601.
- Endo T, Fujii Y, Sugiyama S-I, *et al*. Properties of convective delivery in spinal cord gray matter: laboratory investigation and computational simulations. *J Neurosurg Spine* 2016;24:359–66.
- Ogita S, Endo T, Sugiyama S, *et al*. Convection-enhanced delivery of a hydrophilic nitrosourea ameliorates deficits and suppresses tumor growth in experimental spinal cord glioma models. *Acta Neurochir (Wien)* 2017;159:939–46.
- Yanagisawa M, Kurihara H, Kimura S, *et al*. A novel potent vasoconstrictor peptide produced by vascular endothelial cells. *Nature* 1988;332:411–5.
- Basso DM, Beattie MS, Bresnahan JC. A sensitive and reliable locomotor rating scale for open field testing in rats. *J Neurotrauma* 1995;12:1–21.

- 16 Metz GA, Merkler D, Dietz V, *et al.* Efficient testing of motor function in spinal cord injured rats. *Brain Res* 2000;883:165–77.
- 17 Katahira S, Kawamoto S, Masaki N, *et al.* Oesophageal mucosal blood flow changes after thoracic endovascular stent graft implantation using a novel sensor probe. *Interact Cardiovasc Thorac Surg* 2018;26:487–93.
- 18 Hayatsu Y, Kawamoto S, Matsunaga T, *et al.* Real-time monitoring of spinal cord blood flow with a novel sensor mounted on a cerebrospinal fluid drainage catheter in an animal model. *J Thorac Cardiovasc Surg* 2014;148:1726–31.
- 19 Wang Y, Lin SZ, Chiou AL, *et al.* Glial cell line-derived neurotrophic factor protects against ischemia-induced injury in the cerebral cortex. *J Neurosci* 1997;17:4341–8.
- 20 Die J, Wang K, Fan L, *et al.* Rosuvastatin preconditioning provides neuroprotection against spinal cord ischemia in rats through modulating nitric oxide synthase expressions. *Brain Res* 2010;1346:251–61.
- 21 Fan L, Wang K, Shi Z, *et al.* Tetramethylpyrazine protects spinal cord and reduces inflammation in a rat model of spinal cord ischemia-reperfusion injury. *J Vasc Surg* 2011;54:192–200.
- 22 Schievink WI, Luyendijk W, Los JA. Does the artery of adamkiewicz exist in the albino rat?. *J Anat* 1988;161:95–101.
- 23 Kamada T, Koda M, Dezawa M, *et al.* Transplantation of human bone marrow stromal cell-derived schwann cells reduces cystic cavity and promotes functional recovery after contusion injury of adult rat spinal cord. *Neuropathology* 2011;31:48–58.
- 24 Kajitani T, Endo T, Iwabuchi N, *et al.* Association of intravenous administration of human muse cells with deficit amelioration in a rat model of spinal cord injury. *J Neurosurg Spine* 2021;34:648–55.
- 25 Dewar D, Underhill SM, Goldberg MP. Oligodendrocytes and ischemic brain injury. *J Cereb Blood Flow Metab* 2003;23:263–74.
- 26 Yasuda N, Kuroda Y, Ito T, *et al.* Postoperative spinal cord ischaemia: magnetic resonance imaging and clinical features. *Eur J Cardiothorac Surg* 2021;60:164–74.
- 27 Mazensky D, Flesarova S, Sulla I. Arterial blood supply to the spinal cord in animal models of spinal cord injury. *Anat Rec (Hoboken)* 2017;300:2091–106.
- 28 Saito R, Krauze MT, Bringas JR, *et al.* Gadolinium-loaded liposomes allow for real-time magnetic resonance imaging of convection-enhanced delivery in the primate brain. *Exp Neurol* 2005;196:381–9.
- 29 Arai H, Hori S, Aramori I, *et al.* Cloning and expression of a cDNA encoding an endothelin receptor. *Nature* 1990;348:730–2.
- 30 Sakurai T, Yanagisawa M, Takuwa Y, *et al.* Cloning of a cDNA encoding a non-Isopeptide-selective subtype of the endothelin receptor. *Nature* 1990;348:732–5.
- 31 Kowalczyk A, Kleniewska P, Kolodziejczyk M, *et al.* The role of endothelin-1 and endothelin receptor antagonists in inflammatory response and sepsis. *Arch Immunol Ther Exp (Warsz)* 2015;63:41–52.
- 32 Horinouchi T, Terada K, Higashi T, *et al.* Endothelin receptor signaling: new insight into its regulatory mechanisms. *J Pharmacol Sci* 2013;123:85–101.
- 33 Horie N, Maag A-L, Hamilton SA, *et al.* Mouse model of focal cerebral ischemia using endothelin-1. *J Neurosci Methods* 2008;173:286–90.
- 34 Uchida H, Sakata H, Fujimura M, *et al.* Experimental model of small subcortical infarcts in mice with long-lasting functional disabilities. *Brain Res* 2015;1629:318–28.
- 35 Okada S, Hara M, Kobayakawa K, *et al.* Astrocyte reactivity and astrogliosis after spinal cord injury. *Neurosci Res* 2018;126:39–43.
- 36 Saiki Y, Watanabe K, Ito K, *et al.* Differential selective hypothermic intercostal artery perfusion: a new method to probe spinal cord perfusion during thoracoabdominal aortic aneurysm repair. *Gen Thorac Cardiovasc Surg* 2019;67:180–6.
- 37 Banecki KMRM, Dora KA. Endothelin-1 in health and disease. *Int J Mol Sci* 2023;24:11295.
- 38 Shimada K, Yonetani Y, Kita T, *et al.* Cyclooxygenase 2 expression by endothelin-1-stimulated mouse resident peritoneal macrophages in vitro. *Eur J Pharmacol* 1998;356:73–80.
- 39 Zhu P, Li J, Fujino M, *et al.* Development and treatments of inflammatory cells and cytokines in spinal cord ischemia-reperfusion injury. *Mediators Inflamm* 2013;2013:701970.